

## Interdot carrier transfer in asymmetric bilayer InAs/GaAs quantum dot structures

Yu. I. Mazur,<sup>a)</sup> Zh. M. Wang, G. G. Tarasov,<sup>b)</sup> Min Xiao, and G. J. Salamo  
*Department of Physics, University of Arkansas, Fayetteville, Arkansas 72701*

J. W. Tomm and V. Talalaev  
*Max-Born-Institut für Nichtlineare Optik und Kurzzeitspektroskopie, Max-Born-Strasse 2A,  
 12489 Berlin, Germany*

H. Kissel  
*Ferdinand-Braun-Institut für Höchstfrequenztechnik, Albert-Einstein-Strasse 11, 12489 Berlin, Germany*

(Received 17 September 2004; accepted 7 December 2004; published online 1 February 2005)

Transient photoluminescence from a series of asymmetric InAs quantum-dot bilayers with a GaAs barrier layer thickness varying from 30 to 60 monolayers between the quantum-dot planes is investigated. The interdot carrier transfer process is analyzed. In the framework of a three-level system, interdot carrier transfer times between 200 and 2500 ps are derived and compared with similar data from the literature. Within the semiclassical Wentzel–Kramers–Brillouin approximation, the observed “transfer time-barrier thickness-relation” supports nonresonant tunneling as the microscopic carrier transfer mechanism. © 2005 American Institute of Physics. [DOI: 10.1063/1.1861980]

Semiconductor quantum dots (QDs) are a promising material for various optoelectronic applications.<sup>1</sup> For many practical purposes, such as semiconductor lasers and infrared detectors, three-dimensional QD arrays are needed in order to achieve significant interaction between the optical field and carriers confined within the QDs.<sup>2</sup> As a result, both lateral transport of nonequilibrium carriers within one layer of QDs as well as vertical transport between QD layers is expected to play a significant role in device performance. In previous studies, we have addressed lateral carrier transfer, i.e., the transport of carriers within one QD plane. For this purpose we studied QD structures with a bimodal size distribution and monitored their transient population, in particular the population of larger-sized dots by carriers from smaller-sized QDs, by means of time-resolved photoluminescence (PL).<sup>3,4</sup>

The present study is devoted to the vertical transfer of carriers, i.e., the transport of carriers between two neighboring QD layers along the growth direction. That is, in analogy to our previous work on lateral transport, we report on the transient population of a structure consisting of two QD layers separated by a spacer layer, similar to the structure used in Refs. 5 and 6. By using different InAs deposition rates, growth temperatures, or annealing times for the specific layers, vertically stacked QD layers with differently sized dots, but uniform size distribution in each layer, have been achieved.<sup>7–13</sup> In this case, the spacer thickness between the QD layers represents a very important parameter. In this letter, the population of larger-sized dots (LQD) affected by carriers from smaller-sized dots (SQD) is monitored and transient PL is used as the main tool for the visualization of this inter-QD carrier transfer. In particular, the investigation of a series of asymmetric QD bilayers with barriers of different thicknesses separating the QD layers allows the iden-

tification of the nature of the interdot carrier transfer process as nonresonant tunneling.

The samples studied here are grown using a solid-source molecular beam epitaxy system coupled to an ultrahigh vacuum scanning tunneling microscope (STM). The structures consist of two InAs layers grown on a GaAs(001) substrate, followed by a 0.5  $\mu\text{m}$  GaAs buffer layer. 10 min of annealing at 580 °C provides a nearly defect-free atomically flat surface. The seed, or first QD layer, is fabricated by depositing 1.8 monolayers (ML) of InAs with a growth rate of 0.1 ML/s under an  $\text{As}_4$  partial pressure of  $8 \times 10^{-6}$  Torr at a substrate temperature of 500 °C. GaAs spacer layer ( $d_{\text{sp}}$ ) of 30, 40, 50, or 60 ML was deposited on top of the seed QD layer for each sample, respectively. The second QD layer is then added by deposition of 2.4 ML InAs followed by a 150 ML GaAs cap layer. Structural characterizations are accomplished by plan-view STM and cross-sectional transmission electron microscopy (XTEM). In the seed layer we find a size distribution of  $(4 \pm 1.5)$  nm for the height,  $(20 \pm 3)$  nm for the width, and a dot density of about  $4.5 \times 10^{10} \text{ cm}^{-2}$ . The QD density in the second layer changes over the range of  $(2.5\text{--}4) \times 10^{10} \text{ cm}^{-2}$  depending on the value of  $d_{\text{sp}}$ . The QDs in the second layer are found to have nearly twice the volume of the seed QDs (for  $d_{\text{sp}}=30$  ML). This is due to additional deposition as well as to the influence of the strain field from the seed layer.<sup>5,10,11</sup> Thus, we obtain two vertically correlated QD layers with different sized dots in each layer. Such a system has been called an “asymmetric QD pair” (AQDP) in analogy with extensive work on an asymmetric double quantum-well (ADQW) system.<sup>5</sup> Naturally, the number of QDs in the seed layer participating in the creation of AQDPs must be strongly dependent on the  $d_{\text{sp}}$ . Our XTEM statistical analysis proves this dependence of the AQDP fraction (the correlation degree  $\alpha$ ) on the  $d_{\text{sp}}$  value:  $\alpha=0.95, 0.70, 0.50,$  and  $0.10$  for the  $d_{\text{sp}}=30, 40, 50,$  and  $60$  ML, respectively. A single layer 1.8 ML QD sample is fabricated as well and analyzed as a reference.

<sup>a)</sup>Electronic mail: ymazur@uark.edu

<sup>b)</sup>On leave from Institute of Semiconductor Physics, National Acad. of Sci. of Ukraine, prospect Nauki 45, 03028 Kiev, Ukraine.

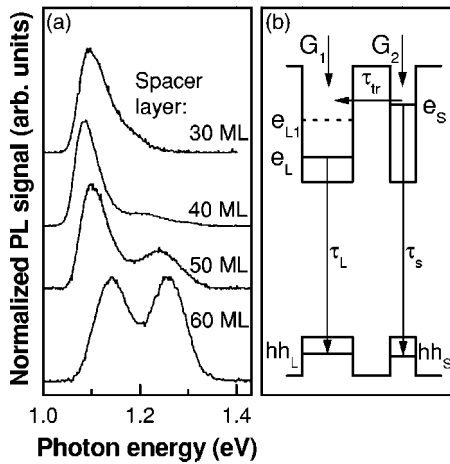


FIG. 1. Steady-state PL spectra at  $T=10$  K for 1.8/2.4 ML samples with various spacer layer thickness. The excitation density is  $0.4 \text{ W cm}^{-2}$ . (b) Schematic representation of processes contributing to carrier dynamics in SQD and LQD ensembles.

Primary characterization of all samples is done by low temperature steady-state PL. Results are given in Fig. 1(a) whereas Fig. 1(b) depicts a simplified energy scheme of the AQDP. As an example, the PL spectrum for the sample with  $d_{sp}=30$  ML shows a single, slightly asymmetric peak at 1.09 eV, corresponding to the expected emission energy from the LQDs in the second layer. With increasing  $d_{sp}$ , however, an additional PL peak at 1.26 eV appears, resulting in a clear double peak structure for the 50 and 60 ML spacer samples. This peak at higher energy agrees well with the PL peak observed for the single 1.8 ML layer reference QD sample. Therefore, it is attributed to the emission of the SQDs in the seed layer. The increasing SQD PL with  $d_{sp}$  can be seen as the first hint for a decreasing carrier transfer probability between the SQDs and LQDs on different layers as one would expect due to the decreased electronic coupling.

Transient PL measurements are performed after impulsive excitation by 80 fs pulses at 732 nm from a mode-locked Ti:sapphire laser operating at 82 MHz. The excitation density is varied between  $10^9$  and  $2 \times 10^{13}$  photons/(pulse  $\times \text{cm}^2$ ) and the signal is detected after passing through a monochromator by a synchro-scan streak camera equipped with an infrared-enhanced S1 cathode. As standard we chose  $5 \times 10^9$  photons/(pulse  $\times \text{cm}^2$ ) as a trade-off between rather low-excitation levels for avoiding excited-state PL contributions and the necessity to achieve a sufficient signal-to-noise ratio. The time resolution of total system is determined to be 15 ps. For all samples, the PL transients of the SQDs are measured at 1.25 eV, at the maximum of the cw PL line assigned to the SQDs, cf. Fig. 1(a). Furthermore, it corresponds to the position of the cw PL maximum of the reference single 1.8 ML QD layer sample as well as to the high energy PL peak caused by the SQDs for the sample with  $d_{sp}=60$  ML, cf. Fig. 1(a) bottom. We believe that the fixation of the PL transients of the SQDs at the position of 1.25 eV in all samples does not noticeably affect the results because we are still within the broad PL maximum of smaller QDs where according to our previous findings the decay time does not change significantly.<sup>3</sup> The spectral window for detecting transient PL from the larger sized dots was chosen between 1.09 and 1.14 eV according to the position of the cw PL peak, cf. Fig. 1(a), left peak. From this point of view, the cw

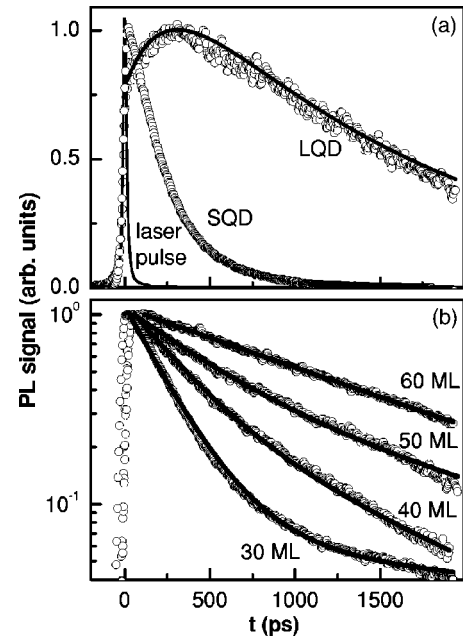


FIG. 2. Normalized PL transients for SQDs and LQDs of an asymmetric QD-bilayer sample with a spacer thickness of 30 ML. The detection energies are at 1.25 and 1.094 eV for SQDs and LQDs, respectively. (b) Normalized PL transients from SQDs of asymmetric QD-bilayer samples. The parameter is the spacer layer thicknesses and the detection energy is at 1.25 eV. The least-squares fit with Eq. (1) is shown as solid lines.

experiments were carried out to carefully locate the PL emission wavelength for the SQDs and the LQDs.

Figure 2(a) gives the normalized PL transient data taken at the PL lines of the AQDP with a spacer thickness of 30 ML. The detection energies are at 1.25 and 1.09 eV for the SQDs and LQDs, respectively. The time-delayed PL from the LQDs convincingly illustrates the refilling of carriers from the SQDs, i.e., by the inter-QD carrier transfer that is addressed in this report. Such behavior may be well understood already within the framework of a three-level system, if the excitation density is chosen adequately low, as is the case here, cf. Ref. 4.

The normalized PL transients from the SQDs for all samples with different  $d_{sp}$  are plotted together in Fig. 2(b). A simple model can be used for the PL-decay time  $\tau_{PL}$  (Ref. 4) and is given by the equation for the SQD PL signal:

$$I(t) = I_0 \{ (1 - \alpha) \exp(-t/\tau_{PL}^{(1)}) + \alpha \exp(-t/\tau_{PL}^{(2)}) \}, \quad (1)$$

where  $\alpha$  is the correlation factor,  $\tau_{PL}^{(1)}$  is the PL decay time for the noncorrelated SQDs in seed layer,  $\tau_{PL}^{(2)}$  is the PL decay time for the correlated SQDs, and

$$\tau_{PL}^{(2)} = \frac{\tau_s \tau_{tr}}{(\tau_s + \tau_{tr})}. \quad (2)$$

Here  $\tau_s$  is the radiative lifetime of nonequilibrium carriers in the SQDs and  $\tau_{tr}$  is the transfer time from the SQDs to the LQDs in AQDPs. For the single layer 1.8 ML QD reference samples we find  $t_{PL}=1.4$  ns. In the following we will use this value for  $\tau_{PL}^{(1)}$  and  $\tau_s$  and, therefore, be able to determine  $\tau_{tr}$  values for all samples if the correlation factor is measured independently. The least squares fit with Eq. (1) is shown in Fig. 2(b) as solid lines. The results are plotted in Fig. 3, with  $\tau_{tr}$  versus the normalized layer thickness (closed circles).<sup>14</sup> In the semilogarithmic plot this dependence is seen to follow a

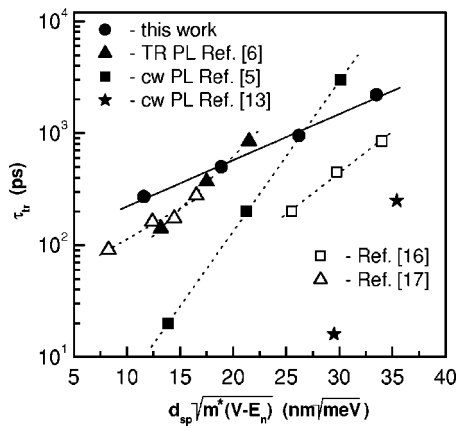


FIG. 3. Inter-QD transfer time vs normalized barrier thickness (closed circles). Data from the literature are added as well. Closed symbols represent data obtained from AQDP (Refs. 5 and 6) whereas open symbols are reference data from asymmetric double QW structures (Refs. 16 and 17).

straight line and pointing to the validity of an expression developed for tunneling processes in coupled QW—the semiclassical Wentzel–Kramers–Brillouin (WKB) approximation. In this approximation  $\tau_{tr}$  is given by

$$\tau_{tr} \propto \exp[2d_{sp}\sqrt{(2m^*/\hbar^2)(V-E_{sn})}]. \quad (3)$$

Here  $m^*$  is the effective mass in the spacer,  $V$  is the band discontinuity of the conduction band,<sup>15</sup> and  $E_{sn}$  represents the lowest confinement energy level in the SQDs. This expression is chosen in order to compare our current results with the results obtained by other authors. In Fig. 3, closed symbols represent data obtained from AQDPs,<sup>5,6</sup> whereas open symbols are reference data from asymmetric double quantum wells (QWs).<sup>16,17</sup>

Note, first that our  $\tau_{tr}$  values exceed all other  $\tau_{tr}$  data and, second, all asymmetric double QD data exceed those of asymmetric double QWs.

The first finding is interpreted as an indication for improved sample quality. In fact, tunneling times are not expected to differ for different samples as long as they are plotted as a function of the quantity  $D = d_{sp}\sqrt{(2m^*/\hbar^2)(V-E_{sn})}$ , accounting for the different material parameters of InAs, GaAs, and AlInAs. In our model, cf. Eq. (2), however,  $\tau_{tr}$  involves all kinds of carrier losses, among others, trapping into defects, in the SQDs, which appear additionally in the AQDP compared to the 1.8 ML QD reference sample.

The second finding is a result of the carrier localization within the QDs. Transfer processes are only possible between QDs right next to each other, whereas for asymmetric double QWs, the free in-plane motion within a QW provides more chances for carriers for finding a location with an empty place on the other side of the barrier.

We should also mention that in our analysis the contribution of the noncorrelated QDs is also taken into account. This fact has been typically ignored during investigations of such transient PL systems.<sup>5,6,13</sup> The noncorrelated QDs contribute on a long time scale. In addition, the correlation factor can be determined independently from XTEM measure-

ments or can serve as a fitting parameter in the least-squares procedure. If one makes  $\alpha$  free the value determined from the optical data fit is only slightly higher ( $\alpha=0.96, 0.74, 0.56,$  and  $0.13$  for the  $d_{sp}=30, 40, 50,$  and  $60$  ML, respectively) than that obtained from XTEM analysis. This is natural while the electronic coupling in AQDP detected through carrier transfer in time-resolved PL measurements is determined not solely by the geometric factors seen in XTEM images.

In summary, we presented a complementary study of the transient PL behavior of a series of AQDPs with different barrier thicknesses between the QD planes. The interdot carrier transfer process is captured and analyzed. Within the semiclassical WKB approximation, the observed “transfer time-barrier thickness-relation” indicates the nonresonant tunneling as the microscopic transfer mechanism.

The authors acknowledge the financial support of the National Science Foundation of US (through Grant Nos. PHY-0099496 and DMR-0080054).

<sup>1</sup>*Semiconductor Quantum Dots: Physics, Spectroscopy and Applications*, edited by Y. Masumoto and T. Takagahara (Springer, Berlin, 2002).

<sup>2</sup>K. Mukai, Y. Nakata, K. Otsubo, M. Sugawara, N. Yokoyama, and H. Ishikawa, *IEEE J. Quantum Electron.* **36**, 472 (2000).

<sup>3</sup>Yu. I. Mazur, J. W. Tomm, V. Petrov, G. G. Tarasov, H. Kissel, C. Walther, Z. Ya. Zhuchenko, and W. T. Masselink, *Appl. Phys. Lett.* **78**, 3214 (2001).

<sup>4</sup>J. W. Tomm, T. Elsaesser, Yu. I. Mazur, G. G. Tarasov, Z. Ya. Zhuchenko, H. Kissel, and W. T. Masselink, *Phys. Rev. B* **67**, 045326 (2003).

<sup>5</sup>R. Heitz, I. Mukhametzhanov, P. Chen, and A. Madhukar, *Phys. Rev. B* **58**, R10151 (1998).

<sup>6</sup>A. Tackeuchi, T. Kuroda, K. Mase, Y. Nakata, and N. Yokoyama, *Phys. Rev. B* **62**, 1568 (2000).

<sup>7</sup>I. Mukhametzhanov, R. Heitz, J. Zeng, P. Chen, and A. Madhukar, *Appl. Phys. Lett.* **73**, 1841 (1998).

<sup>8</sup>M. O. Lipinski, H. Schuler, O. G. Schmidt, K. Eberl, and N. Y. Jin-Phillipp, *Appl. Phys. Lett.* **77**, 1789 (2000).

<sup>9</sup>P. B. Joyce, E. C. Le Ru, T. J. Krzyzewski, G. R. Bell, R. Murray, and T. S. Jones, *Phys. Rev. B* **66**, 075316 (2002).

<sup>10</sup>Yu. I. Mazur, X. Wang, Z. M. Wang, G. J. Salamo, M. Xiao, and H. Kissel, *Appl. Phys. Lett.* **81**, 2469 (2002).

<sup>11</sup>Yu. I. Mazur, Z. M. Wang, G. J. Salamo, M. Xiao, G. G. Tarasov, Z. Ya. Zhuchenko, W. T. Masselink, and H. Kissel, *Appl. Phys. Lett.* **83**, 1866 (2003).

<sup>12</sup>J. He, Y. C. Zhang, B. Xu, and Z. G. Wang, *J. Appl. Phys.* **93**, 8898 (2003).

<sup>13</sup>E. C. Le Ru, P. Howe, T. S. Jones, and R. Murray, *Phys. Rev. B* **67**, 165303 (2003).

<sup>14</sup>Comment on the mechanisms underlying interdot carrier transfer: In contrast to the asymmetric double QW structures, in the vertically aligned AQDP the three-dimensional shape of the InAs dots makes the definition of  $d_{sp}$  somewhat arbitrary. The uniformity of the dots leads to statistical variations, especially in the case of weakly correlated QD pairs, which require introducing an effective tunnel barrier thickness defined as the average distance between the top of the SQDs and the bottom of the LQDs. In Fig. 3, we use the effective  $d_{sp}$  by taking into account the average QD height of  $\sim 4$  nm determined from STM images of the uncapped single 1.8 ML sample (Refs. 10 and 11).

<sup>15</sup>N. Horiguchi, T. Futatsugi, Y. Nakata, N. Yokoyama, T. Mankad, and P. M. Petroff, *Jpn. J. Appl. Phys., Part 1* **38**, 2559 (1999).

<sup>16</sup>T. H. Wang, X. B. Mei, C. Jiang, Y. Huang, J. M. Zhou, X. G. Huang, C. G. Cai, Z. X. Yu, C. P. Luo, J. Y. Xu, and Z. Y. Xu, *Phys. Rev. B* **46**, 16160 (1992).

<sup>17</sup>D. H. Levi, D. R. Wake, M. V. Klein, S. Kumar, and H. Morkoç, *Phys. Rev. B* **45**, 4274 (1991).